Low energy (e,2e) measurements of CH4 and neon in the perpendicular plane

Kate L. Nixon, Andrew James Murray, Hari Chaluvadi, Sadek Amami, Don H. Madison et al.

Citation: J. Chem. Phys. **136**, 094302 (2012); doi: 10.1063/1.3690461
View online: http://dx.doi.org/10.1063/1.3690461
View Table of Contents: http://jcp.aip.org/resource/1/JCPSA6/v136/i9
Published by the American Institute of Physics.

Low energy (e,2e) measurements of CH_4 and neon in the perpendicular plane

Kate L. Nixon,[1,a)] Andrew James Murray,[1] Hari Chaluvadi,[2] Sadek Amami,[2] Don H. Madison,[2] and Chuangang Ning[3]
[1]*Photon Science Institute, School of Physics and Astronomy, University of Manchester, Oxford Road, Manchester M13 9PL, United Kingdom*
[2]*Department of Physics, Missouri University of Science and Technology, Rolla, Missouri 65409, USA*
[3]*Department of Physics, State Key Laboratory of Low-Dimensional Quantum Physics, Tsinghua University, Beijing 100084, People's Republic of China*

(Received 11 January 2012; accepted 10 February 2012; published online 1 March 2012)

Low energy experimental and theoretical triple differential cross sections for the highest occupied molecular orbital of methane ($1t_2$) and for the 2p atomic orbital of neon are presented and compared. These targets are iso-electronic, each containing 10 electrons and the chosen orbital within each target has p-electron character. Observation of the differences and similarities of the cross sections for these two species hence gives insight into the different scattering mechanisms occurring for atomic and molecular targets. The experiments used perpendicular, symmetric kinematics with outgoing electron energies between 1.5 eV and 30 eV for CH_4 and 2.5 eV and 25 eV for neon. The experimental data from these targets are compared with theoretical predictions using a distorted-wave Born approximation. Reasonably good agreement is seen between the experiment and theory for neon while mixed results are observed for CH_4. This is most likely due to approximations of the target orientation made within the model. © *2012 American Institute of Physics*. [http://dx.doi.org/10.1063/1.3690461]

I. INTRODUCTION

Electron impact ionisation collisions at low energies are important in a number of fundamental areas. These include plasma etching in industry, to the study of natural atmospheric phenomena as well as cancer therapy by radiation treatments. In order to understand the underlying physical process in these areas, a robust understanding of the collision is necessary. Experimental measurements provide data for specific collision parameters from a particular target. By developing comprehensive theoretical models of the collision that are rigorously tested by experiment, accurate predictions for a range of collision parameters from a multitude of targets can then be made. Precise experimental data are hence required to aid in the development of the theoretical models.

(e,2e) experiments control the projectile electron momentum and define the momentum of the electrons resulting from the collision. As such, these kinematically complete experiments provide the most detailed data against which theory can be compared. This field has provided a rich source of information on atomic targets, with good agreement being found between experiment and theory for a range of different atoms. By contrast, the number of molecules that have been investigated is still relatively small, and new models are currently under development. This is due to the more complex nature of molecules compared to atoms. Molecules have spatially distributed nuclei resulting in multiple scattering centres, which means that the wave-functions associated with the electron distribution within the molecule are not spherically symmetric. This reduction in symmetry leads to further complications, since the orientation and alignment of the molecule with respect to the scattering geometry must also be considered. Additionally, the energy levels within molecules are often more closely spaced than in atoms, resulting in neighbouring orbitals that may not be resolvable by experiment. Despite these theoretical and experimental challenges, detailed electron impact ionisation studies from molecules have been emerging over the past decade.

The molecular target in this current study is methane (CH_4), which is the smallest hydrocarbon and so is a relatively simple molecule. It has five atoms, with ten electrons. The molecule has tetrahedral symmetry and only two valence energy levels. The $1t_2$ level is the highest occupied molecular orbital (HOMO) and is a triply degenerate, p-like orbital. The next highest occupied molecular orbital ($2a_1$) has almost spherical symmetry, and has s-like character. These orbitals are separated in energy by ~9 eV, allowing data to be obtained from the individual orbitals without contamination. Recent measurements from CH_4 using scattered electron energies of 500 eV have been reported[1] and corresponding distorted-wave Born approximation (DWBA) calculations[2] show good agreement at these higher energies. The data presented here are low energy triple differential cross sections (TDCS) using symmetric energy sharing, where both outgoing electrons leave the collision with equal energy. Perpendicular kinematics were used in which the momentum of the incident projectile electron is orthogonal to the detection plane containing the two outgoing electrons (see Figure 1). In order for both outgoing electrons to leave the collision in this plane, it is necessary for multiple scattering to occur. This geometry hence provides a stringent test of theory. Additionally,

a)Author to whom correspondence should be addressed. Electronic mail: kate.nixon-2@manchester.ac.uk.

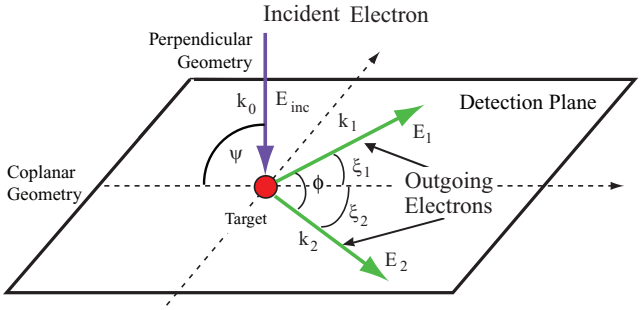

FIG. 1. Diagram of the geometry used in this study. A perpendicular geometry ($\psi = 90°$) is defined when the momentum of the incident electron is perpendicular to that of the outgoing electrons, i.e., the detection plane. In the perpendicular geometry only the mutual angle ($\phi = \xi_1 + \xi_2$) is relevant.

marked differences have been observed between atomic helium and molecular H_2 in this plane, in contrast to results taken in a coplanar geometry where the cross sections were similar.[3] Since He and H_2 have the same number of electrons and protons, these results indicate that measurements in the perpendicular plane provide a more sensitive test of the structure of the target than data taken in a coplanar geometry.

To further understand the measurements from CH_4, the resulting TDCS is compared with that from neon. Neon is the iso-electronic atom to CH_4, both species having 10 electrons. By comparing the atomic and molecular cross sections, similarities in the TDCS may be attributable to a similar electronic structure, while differences may arise due to the molecular nature of the target.

A previous study from the NHOMO ($2a_1$) orbital of CH_4 in a coplanar geometry yielded poor statistical accuracy due to very low signal at these energies,[4] and so the TDCS for the outermost orbital of the two species are presented here, i.e., the $1t_2$ orbital of CH_4 and the corresponding 2p orbital of Ne.

This paper is structured as follows. Section II describes the pertinent details of the apparatus used to collect the data. The theoretical framework used to model the collision is then detailed in Sec. III. Results from experimental measurement and theoretical predictions are presented and discussed in Sect. IV. Section V summarises this study and maps out future work that is needed.

II. EXPERIMENTAL APPARATUS

The fully computer controlled and computer optimised (e,2e) spectrometer at the University of Manchester was used in this work. This apparatus has been described elsewhere[5] so only the salient points are discussed here. The spectrometer consists of an electron gun with an energy resolution of ~600 meV, two electron analysers, a gas jet and a Faraday cup. The electron analysers are mounted on individual turntables so that they can be independently rotated around the interaction region. The detection plane is defined by these analysers (see Figure 1). In this study the spectrometer was configured in a perpendicular geometry where the momentum of the incident electron is perpendicular to the detection plane ($\psi = 90°$). The data are symmetric as the outgoing electrons were detected with equal energies, i.e., $E_1 = E_2$, and the only angle of relevance in this plane is the angle between the analysers, $\phi = \xi_1 + \xi_2$.

High purity CH_4 or neon was admitted into the interaction region through a gas jet. The flow of the target gas was controlled by a needle valve. Typical operating pressures for CH_4 and Ne were 1.2×10^{-5} Torr and 2.2×10^{-5} Torr, respectively. Small incident electron beam currents, typically ~120 nA, were used for CH_4 in order to maintain a good signal to background ratio. Higher currents of 300 nA were used for neon.

The spectrometer was operated under computer control throughout data collection. The electrostatic lenses in the analysers were optimised at each new angle to ensure maximum signal. The energy of the incident electron beam was calibrated at the beginning of each new data set by locating the peak in the coincidence binding energy spectrum. The two highest occupied molecular orbitals of CH_4 are well separated by ~9 eV. The experimental energy resolution of ~1.4 eV easily ensures there is no contamination in the measured data from the neighbouring orbital, as is often the case for molecular targets.[6–8]

The data have not been placed on an absolute scale due to the low energies used in this study. Molecular targets may have a dramatic influence on the behaviour of the electron beam at these energies[9] and so it is not accurate to assume that the electron beam density remains constant between measurements as the energy is changed or for different target species, as is essential in the normalisation methods applied by others at higher energies.[10,11] Consequently, the data presented here are normalised to unity at the highest data point for each set. Each data set is generated from an average of many sweeps around the detection plane. The error bars on the TDCS represent the standard error derived from this average. The uncertainties on the scattering angle are due to the pencil angle of the incident electron beam, and the acceptance angles of the outgoing electron analysers. This is estimated to be $\pm 5°$.

The experimental data for neon have been published previously.[12] The data are re-presented here so that a direct comparison can be made between the two iso-electronic species.

III. THEORETICAL FRAMEWORK

The molecular 3-body distorted wave (M3DW) approximation [or atomic 3-body distorted wave (3DW) approximation] has been detailed in previous publications[13–15] so only a brief outline is given here. The TDCS for the M3DW is giving by

$$\frac{d^5\sigma}{d\Omega_a \Omega_b dE_b} = \frac{1}{(2\pi)^5}\frac{k_a k_b}{k_i}|T|^2, \tag{1}$$

where $\vec{k}_i$, $\vec{k}_a$, and $\vec{k}_b$ are the wave vectors for the initial, scattered, and ejected electrons. The scattering amplitude is given by

$$T = \langle \chi_a^-(\vec{k}_a, \mathbf{r}_1)\chi_b^-(\vec{k}_b, \mathbf{r}_2)C_{scat-eject}(r_{12}^{ave})|V - U_i|\phi_{DY}^{OA}(\mathbf{r}_2)\chi_i^+(\vec{k}_i, \mathbf{r}_1)\rangle, \tag{2}$$

where r_1 and r_2 are the coordinates of the incident and bound electrons, χ_i, χ_a, and χ_b are distorted waves representing the incident, scattered, and ejected electrons, respectively, and $\phi_{DY}^{OA}(r_2)$ is the initial bound-state Dyson molecular orbital averaged over all orientations. The molecular wave-functions were calculated using density functional theory along with the standard hybrid B3LYP (Ref. 16) functional by means of the ADF 2007 (Amsterdam Density Functional) program[17] with the TZ2P (triple-zeta with two polarization functions) Slater type basis sets. For the $1t_2$ state, the average of the absolute value of the Dyson wave-function is taken prior to the collision, since the normal average is zero due to parity of the wave-function.[4]

For the Ne atom, the same matrix element (2) is evaluated except the Dyson orbital is replaced by a Hartree-Fock 2p wave-function. The factor $C_{scat-eject}(r_{12}^{ave})$ is the Ward-Macek average Coulomb-distortion factor between the two final state electrons,[18] V is the initial state interaction potential between the incident electron and neutral molecule, and U_i is a spherically symmetric distorting potential which is used to calculate the initial-state distorted wave for the incident electron $\chi_i^+(\vec{k}_i, \mathbf{r}_1)$.

The Schrödinger equation for the incoming electron wave-function is given by

$$\left(T + U_i - \frac{k_i^2}{2}\right)\chi_i^+(\vec{k}_i, r) = 0, \tag{3}$$

where T is the kinetic energy operator and the "+" superscript on $\chi_i^+(\vec{k}_i, \mathbf{r})$ indicates outgoing wave boundary conditions. The initial state distorting potential contains three components $U_i = U_s + U_E + U_{CP}$. U_s is the static potential that contains the nuclear contribution and a spherically symmetric approximation for the interaction between the projectile electron and the target electrons which is obtained from the quantum mechanical charge density of the target. U_E is the exchange potential of Furness-McCarthy (corrected for sign errors) (Ref. 19) which approximates the effect of the continuum electron exchanging with the passive bound electrons in the molecule. Finally, U_{CP} is the correlation-polarization potential of Perdew and Zunger,[20] and Padial and Norcross.[21]

The final state for the system is approximated as a product of distorted waves for the two continuum electrons multiplied by the average Coulomb-distortion factor. The final state distorted waves are calculated as the initial state, except that the final state spherically symmetric static distorting potential for the molecular ion (or atomic ion) is used for U_s.

IV. RESULTS

A. Predicted scattering signatures using a classical model

A recent investigation by Al-Hagan *et al.*[3] considers a simple classical picture of the ionisation of atoms and molecules in the perpendicular plane that is validated using quantum mechanical calculations. These authors provide an explanation for features observed in the measured cross sections when the experiments do not determine the orientation of a molecular target. Predictions were given for (i) atomic targets, (ii) molecular targets that have a nucleus at the centre of mass, and (iii) molecular targets that do not have a nucleus at the centre of mass. Experimental and theoretical data from He, H_2, and CO_2 with $E_1 = E_2 = 10$ eV were used in their study. It was predicted that molecules with no nucleus at the centre of mass should produce a minimum contribution to the cross section at angles corresponding to the outgoing electrons emerging back to back, i.e., at $\phi = 180^\circ$. This prediction results from the model averaging over all possible orientations of the molecule prior to the collision (as is adopted in the calculations used in this paper), so that the nuclear charge appears as a thin "shell" of charge with a diameter set by the inter-nuclear distance. In these averaging models, electrons that collide inside the resulting nuclear shell cannot experience any force from the nuclei, and so only a binary collision will occur (no re-collision from the nucleus then being possible). In this case the TDCS in the perpendicular plane should only present peaks at $\phi \sim 90^\circ, 270^\circ$, as was observed for H_2. The model further suggests that molecular targets that *do* have a nucleus at the centre of mass should then yield a backscattering signature similar to atomic targets, since nuclear re-scattering can then occur. This prediction was confirmed in their data for CO_2, which produced a TDCS similar in structure to that of helium, with peaks at $\phi \sim 90^\circ, 270^\circ$ (due to binary collisions) and a third peak at 180° (due to re-scattering of one of the electrons from the nucleus). Since CH_4 has a carbon atom at the centre of mass of the molecule, this simple classical model predicts that CH_4 should produce a 3-peak TDCS, with significant cross section at $\phi = 180^\circ$.

B. 2p orbital of neon

The experimental and theoretical TDCS for the valence 2p orbital of neon are shown in Figure 2. The theoretical data have been calculated in the DWBA framework. Two curves are shown that represent different calculations. The first is a basic DWBA calculation (DWBA). The second (3DW) has post-collisional interactions (PCI) included by using the Ward-Macek approximation.[18] The result of an independent theoretical study by Purohit *et al.*[22] is also shown for an incident electron energy 20 eV above the ionisation potential.

The structure of the data has been discussed previously.[12] Briefly, a double peak structure is observed at high energies, with a *minimum* at $\phi = 180^\circ$ in contrast to both the prediction of the simple model described in Sec. IV A, and the experimental results from helium.[12] As the energy decreases the two peaks move closer together giving a narrower distribution, and the local minimum at $\phi = 180^\circ$ becomes shallower. At the lowest energy studied here ($E_1 = E_2 = 2.5$ eV), a single peak is observed. This peak will include a contribution due to PCI between the two outgoing electrons,[23] since at these low energies the longer interaction time between the outgoing electrons results in them asymptotically being driven apart.

It is interesting that the simple classical picture[3] already appears to fail for this target. The absence of a defined peak at $\phi = 180^\circ$ may be attributable to the proposed nuclear re-scattering mechanism having a much smaller probability than for helium, compared with the binary mechanism that gives

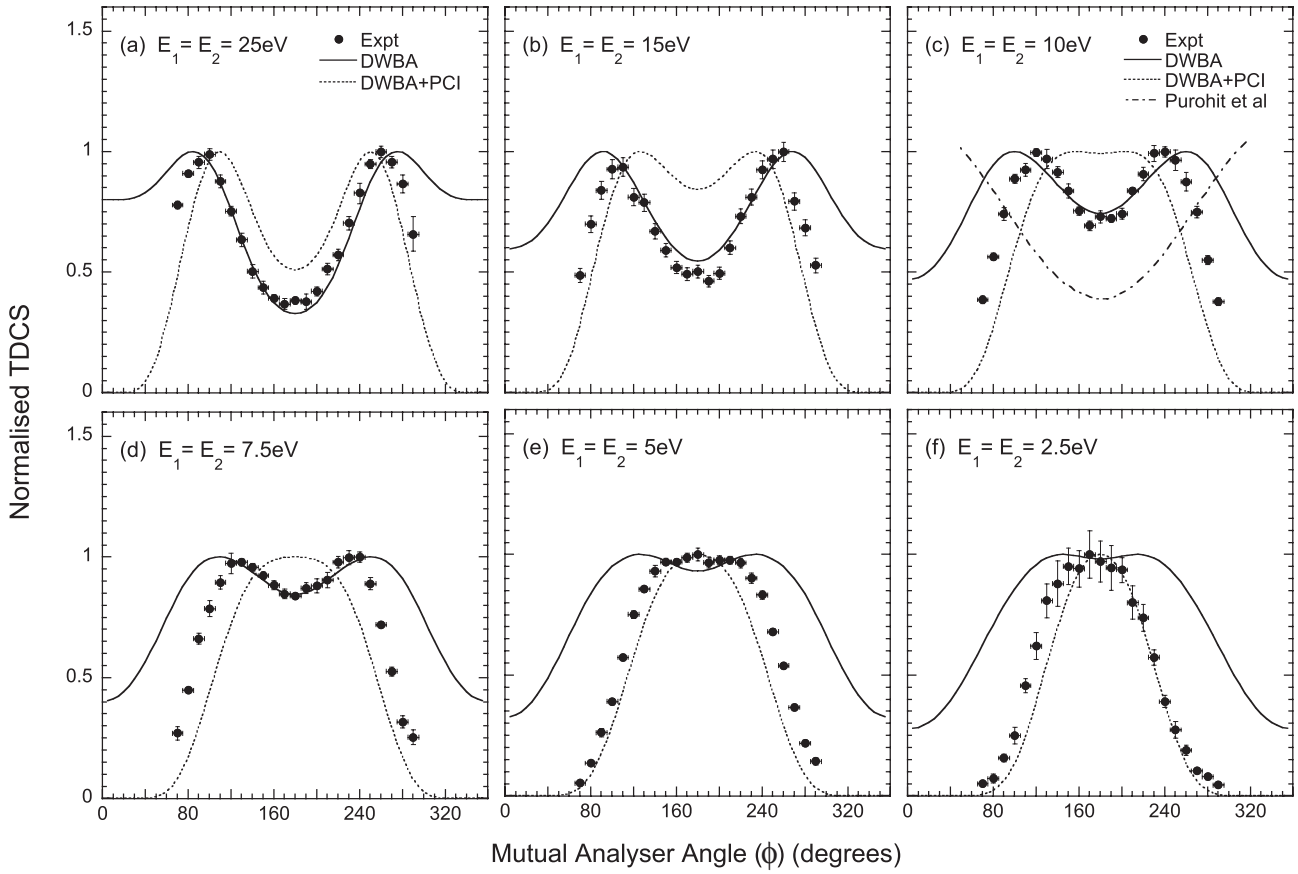

FIG. 2. Experimental and theoretical TDCS for the 2p orbital of neon. Incident energies of 5 eV to 50 eV above the ionisation potential (IP = 21.6 eV) were used, as indicated on the plots. Two theoretical predictions are shown for all energies; DWBA with no PCI included (solid line) and 3DW (dashed line) where PCI is treated using the Ward-Macek approximation. An additional theoretical curve is shown in (c) following the calculation of Purohit *et al.*[22] The experimental and theoretical data have been independently normalised to unity at the peak of the TDCS for each energy.

rise to the peaks on either side. This hypothesis is strengthened by the 3DW model that also predicts a minimum at $\phi = 180^\circ$, in agreement with the data. From a classical viewpoint, it would be expected that nuclear scattering would be weaker for neon since the classical impact parameters for elastic scattering into the perpendicular plane would be five times larger for neon than helium. Consequently, it appears that the physical effects leading to the shape of the cross section is different for this case. The fact that both the DWBA and 3DW predict a minimum at 180° indicated that the minimum is not related to the electron–electron interaction in the final state.

The prediction from the DWBA calculation (i.e., without PCI) shows unphysically high flux when the electrons emerge at the same angle, i.e., at the mutual angles $\phi = 0^\circ$ and $\phi = 360^\circ$. This clearly shows the importance of PCI, as is included in the 3DW prediction. PCI can also be attributed to the narrowing of the TDCS around $\phi = 180^\circ$ as the energy is lowered. This reduction in width is due to the electrons that emerge from the interaction region repelling each other.

The correlation between experimental data and the theoretical predictions is interesting. At high energy, the DWBA calculation predicts the depth of the minimum at $\phi = 180^\circ$ with more accuracy than the 3DW calculation, which also predicts too narrow a distribution at these energies. This may indicate that the contribution due to PCI is too strong in the model. Conversely, at the lowest energy the 3DW calculation is far more successful at predicting the width of the distribution. Neither model emulates the success that was found for helium.

In addition to the predictions given here, Figure 2(c) also shows the DWBA calculation by Purohit *et al.*[22] This calculation used a spin averaged static exchange potential, includes PCI via the Gamow factor and employs a polarization potential in the incident channel only. Only one calculation for neon in the perpendicular plane was reported by these authors, at outgoing electron energies $E_1 = E_2 = 10$ eV. Their calculation predicts a minimum at $\phi = 180^\circ$, as is observed. By contrast, their predicted cross section increases in both directions towards $\phi = 0^\circ$ and $\phi = 360^\circ$, and their minimum is broader and deeper than is seen in the experimental data.

C. $1t_2$ state of methane

The experimental and theoretical TDCS for the HOMO of CH_4 (the $1t_2$ state), are shown in Figures 3 and 4. Figure 3 compares the data to the DWBA model, whereas Figure 4 shows a comparison with the M3DW model. The HOMO of CH_4 is a triply degenerate state consisting of three p-like orbitals. These orbitals have parity inversion through the centre of symmetry, which is also the centre of mass in CH_4. To allow for parity inversion, the present models use

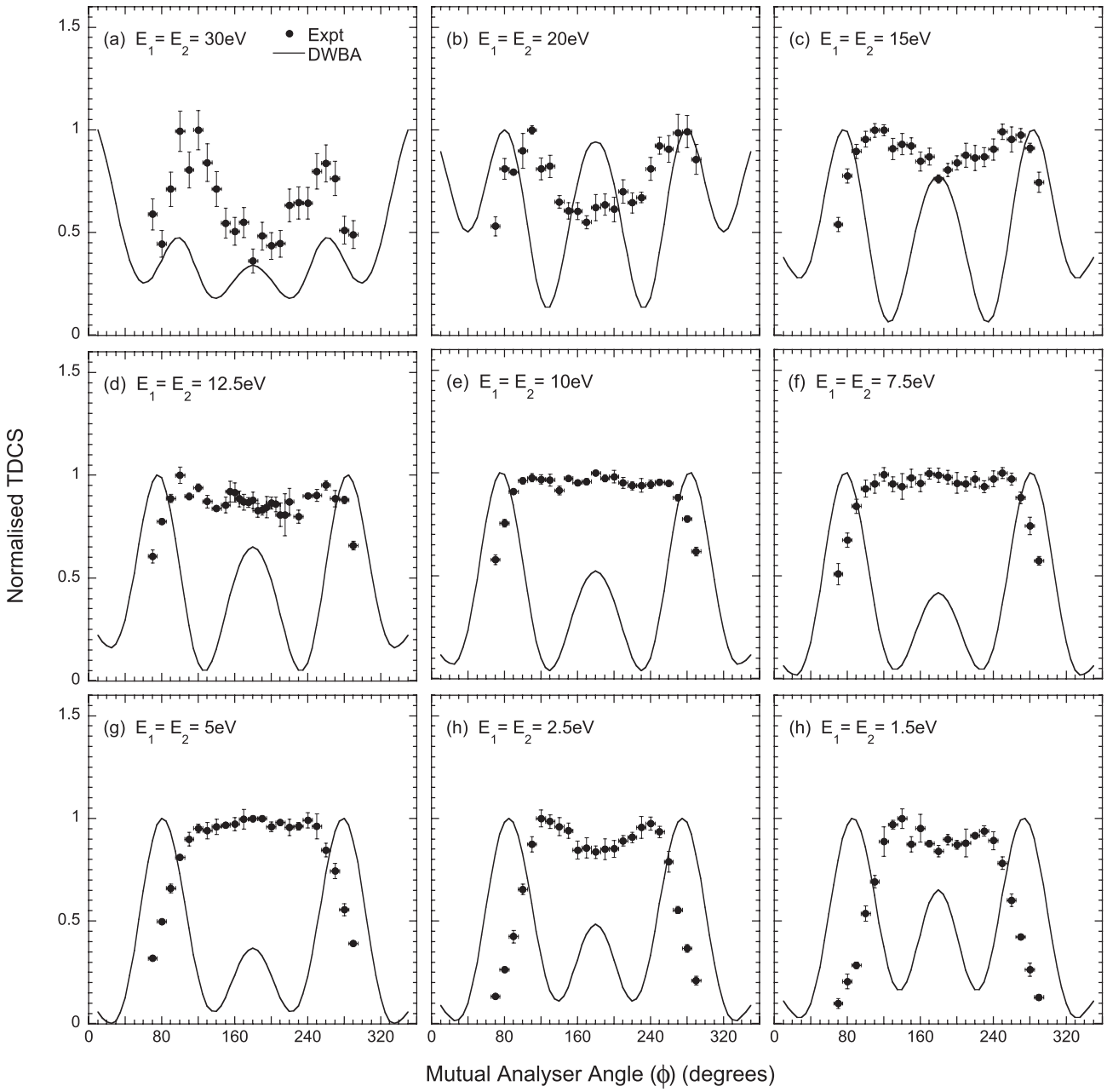

FIG. 3. Experimental and theoretical DWBA TDCS for the $1t_2$ HOMO state of CH_4. Incident energies of 3 eV to 60 eV above the ionisation potential (IP ~ 14 eV) were used, as indicated on the plots. The experimental and theoretical data have been independently normalised to unity at the peak for each energy.

the absolute value of the orbital wave-function to generate an averaged wave-function over all orientations of the molecule. This is used here since the averaging procedure would produce a zero wave-function if parity inversion was included. It has been found that the orientationally averaged molecular wave-function used for this state is of reasonably good quality[4] when compared with experimentally measured EMS data[24] at high energies.

The data show a two-peak structure at the highest energy used here, i.e., $E_1 = E_2 = 30$ eV as shown in Figures 3(a) and 4(a). The peaks are located symmetrically about $\phi = 180°$, at angles of $\phi = 110°$ and $\phi = 260°$. A minimum is observed between the two peaks with a magnitude ~0.45 of the peaks. This is similar to that observed for the valence states of neon, argon, and krypton.[12] As the energy of the outgoing electrons is decreased, the two peaks remain approximately in the same position and the local minimum fills in. In figures (d)–(g), the distribution is wide, flat, and almost featureless. Evidence of a faint triple peak structure may be observed. As the energy is lowered further the total angular width of the cross section decreases, and a small two-peak structure is again seen at the two lowest energies. Here, the two peaks are found at $\phi = 120°$ and $\phi = 240°$, and the minimum at $\phi = 180°$ has an intensity ~0.85 of the peak height.

Both DWBA and M3DW models predict well-resolved triple peak structures at the majority of energies measured. The peak at $\phi = 180°$ seen in the theoretical results emulates the prediction of the classical model described in Al-Hagan *et al.*[3] Initially consider the DWBA prediction as in Figure 3. At high energies the calculation shows unphysical intensity

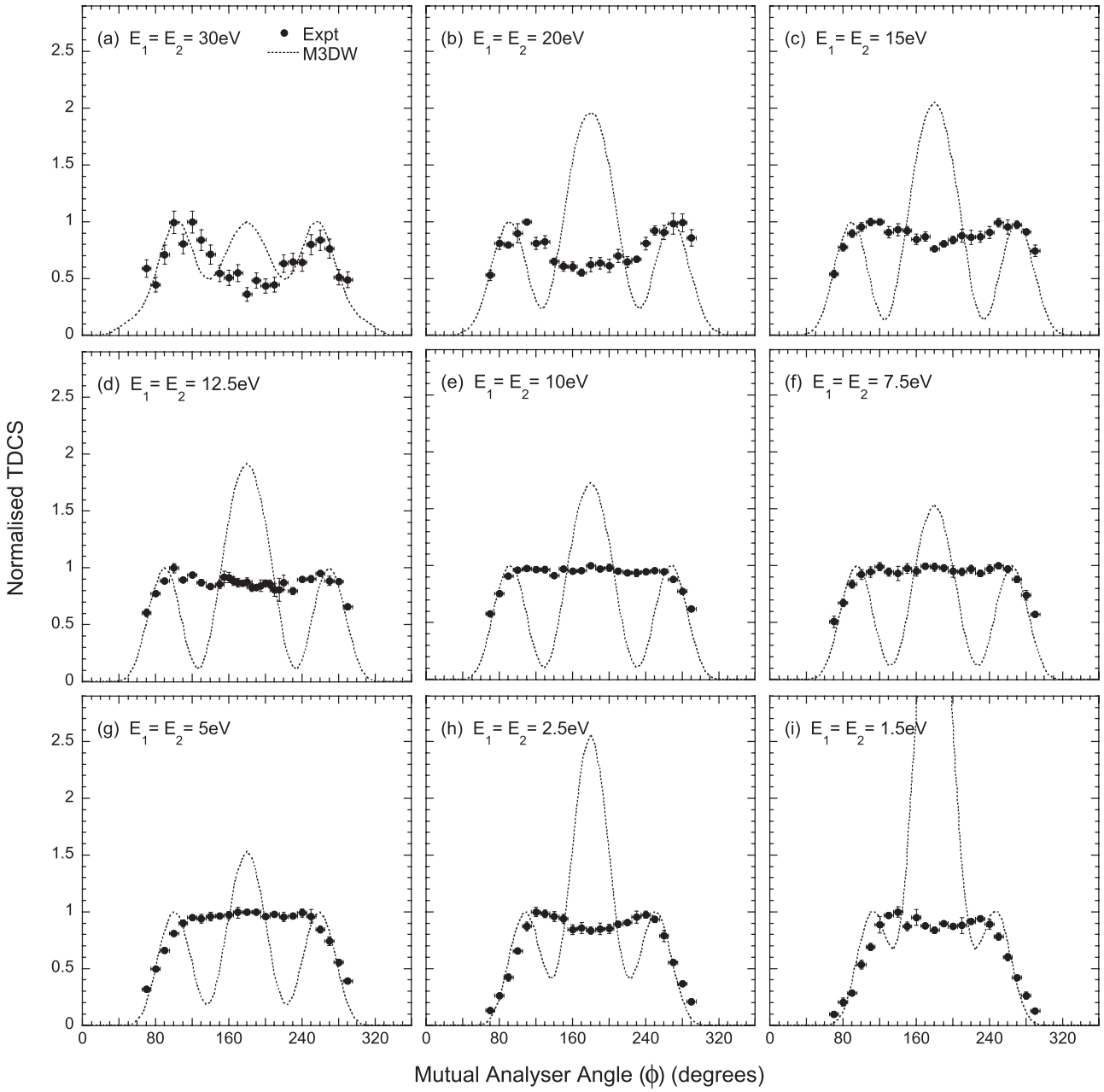

FIG. 4. Experimental and theoretical (M3DW) TDCS for the $1t_2$ HOMO state of CH_4. The experimental data have been normalised to unity at the maximum intensity, while the theoretical data are normalised to unity at the side peaks. For details, see text.

at $\phi = 0^\circ$ and 360°, which is due to the absence of PCI in the model, as seen for neon in Figure 2. The model predicts a triple peak structure at the lower energies, the width of the cross section being overestimated at almost all energies by this calculation.

The predictions from the M3DW calculation that includes PCI using the Ward-Macek approximation[18] are shown in Figure 4. In this figure the data are normalised to unity at the two side peaks. The agreement in width of the TDCS between experiment and theory is much more satisfactory for all energies, and the unphysical cross section at $\phi = 0^\circ$ and 360° is now eliminated due to inclusion of PCI. There is, however, a discrepancy in the number of peaks that are predicted, and the large relative magnitude of the TDCS at $\phi = 180^\circ$ predicted by the model is not observed.

Once again, the TDCS generated by this model is in good agreement with that expected from the classical model outlined in Sec. IV A, with three clearly defined peaks and with a large central peak at $\phi = 180^\circ$ (as observed for helium). The magnitude of the predicted peak at $\phi = 180^\circ$ indicates that rescattering from the carbon nucleus is much stronger than for the iso-electronic neon atom at similar energies. This probably results from the fact that the classical impact parameters for elastic scattering into the perpendicular plane are smaller for the molecule than they are for the atom.

A similar discrepancy regarding the number of discrete peaks predicted by theory was noted for H_2O in the perpendicular plane.[9] In these experiments the excess energy remained constant at 20 eV and the energy sharing between the two outgoing electrons was varied. In the three cases studied

for this target, the experimental distribution was relatively flat as is seen here for CH_4, in contrast to theory that predicted a well-defined triple peak structure.

D. Comparison between the iso-electronic species

The experimental distributions for the two iso-electronic analogues neon and CH_4, show some similarities in the shape of the cross section. Differences, particularly at intermediate and low energies, are also observed. To summarise; at high energies both targets display a double peak structure. Also, in both cases the local minimum is filled in as the energy is decreased. For neon, the width of the distribution narrows as the energy is lowered, and the angular distribution shows a small flat section at $E_1 = E_2 = 5$ eV where the TDCS transitions between a double peak structure and a single peak. In contrast, the width of the CH_4 distribution remains essentially constant until $E_1 = E_2 = 5$ eV. The TDCS of CH_4 is relatively flat and featureless over the range of outgoing electron energies from 12.5 eV to 5 eV, while the distributions for neon always show a double peak structure until $E_1 = E_2 = 5$ eV. At the lowest energies used here, neon presents a single peak, while CH_4 shows a shallow double peak structure. At these energies the width of the CH_4 distribution starts to reduce.

Comparison with the theoretical results for these two species show large differences. For all but the lowest energy, a minimum is predicted at $\phi = 180^\circ$ for neon. Conversely, a maximum is predicted at $\phi = 180^\circ$ for CH_4. Indeed, this maximum dominates the predicted TDCS when PCI is included, in contrast to what is observed in the experiment.

V. CONCLUSIONS

In comparing the theoretical predictions for neon to the data, it is seen that neither the DWBA nor the 3DW models provide an accurate description over the entire energy range investigated here. At high energies the DWBA model accurately predicts the depth of the minimum at $\phi = 180^\circ$, but overestimates the width of the distribution. At low energies inclusion of PCI narrows the width around $\phi = 180^\circ$ so as to be in reasonably good agreement with the data, as is expected. In a similar way, inclusion of PCI for CH_4 narrows the width of the distribution. This produces good agreement with the width of the distribution over all energies, although a large peak at $\phi = 180^\circ$ is predicted that is not observed.

Much better agreement between experiment and theory is found for Ne than CH_4. CH_4 is clearly a more complex target than neon. This additional complexity is reflected in the evolution of the TDCS with energy. The data for neon shows a double peak at high energies that narrows to a single peak as the energy is lowered. The 3DW calculation shows the same transition, except the single peak occurs at a higher energy than experiment. The TDCS for CH_4 also starts with a double peak at high energies. The total angular width of the distribution however remains unchanged until $E_1 = E_2 = 5$ eV at which point the width decreases. The M3DW correctly predicts the width of the peak for all energies. As the energy is lowered however, the experimental minimum at $\phi = 180^\circ$ fills in to yield a broad, flat topped distribution while the M3DW predicts a maximum at $\phi = 180^\circ$ which becomes larger with decreasing energy.

The most obvious discrepancy between data and theory is the number of clearly resolved peaks predicted for CH_4. The peak at $\phi = 180^\circ$ is predicted to be significantly enhanced in the M3DW model in contrast to what is observed. There is perhaps a small triple peak between E = 12.5 eV and 7.5 eV in the data, however this is poorly defined. It would be interesting to investigate if the featureless cross section in the data is due to an incoherent summation of cross sections from the different molecular orientations that occur in the experiment, or if it is due to a quantum mechanical effect that is not being reproduced in the theory. To establish this, the model needs to calculate the TDCS for different orientations of the target *prior* to the collision, and then average the resulting cross sections over all possible orientations of the target. This is a challenging and computationally intensive calculation, however it would provide the most accurate comparison with the data, and would most accurately test the models that are being developed.

In conclusion, it is clear that much has yet to be done to resolve the differences that are seen between theory and experiment at these incident energies. It is important to establish a robust theory for collisions with molecules at these energies since it is here that the cross section for ionization is highest, and so it is in this energy regime where most collisions occur in nature. The contrasts that have been observed between the iso-electronic targets of neon and CH_4 show that conclusions can be made about the nature of the collision for molecular targets. It is clear however that a full calculation that does not include orientation averaging prior to the collision is now required.

ACKNOWLEDGMENTS

This work was supported by the U.S. National Science Foundation (NSF) under Grant. No. PHY-1068237. The author C.N. would like to acknowledge the support of the National Natural Science Foundation of China (NNSFC) under contract No. 10704046. K.L.N. would like to thank the Royal Society for a Newton International Fellowship held at the University of Manchester.

[1] A. Lahmam-Bennani, A. Naja, E. M. Staicu Casagrande, N. Okumus, C. Dal Cappello, I. Charpentier, and S. Housamer, J. Phys. B **42**, 165201 (2009).
[2] I. Toth and L. Nagy, J. Phys. B **43**, 135204 (2010).
[3] O. Al-Hagan, C. Kaiser, D. H. Madison, and A. J. Murray, Nat. Phys. **5**, 59 (2009).
[4] K. L. Nixon, A. J. Murray, H. Chaluvadi, C. Ning, and D. H. Madison, J. Chem. Phys. **134**, 174304 (2011).
[5] A. J. Murray, B. C. H. Turton, and F. H. Read, Rev. Sci. Instrum. **63**, 33465 (1992).
[6] C. J. Colyer, S. M. Bellm, B. Lohmann, G. F. Hanne, O. Al-Hagan, D. H. Madison, and C. G. Ning, J. Chem. Phys. **133**, 124302 (2010).
[7] C. J. Colyer, M. A. Stevenson, O. Al-Hagan, D. H. Madison, C. G. Ning, and B. Lohmann, J. Phys. B **42**, 235207 (2009).
[8] A. Naja, E. M. Staicu-Casagrande, A. Lahmam-Bennani, M. Nekkab, F. Mezdari, B. Joulakain, O. Chuluunbaatar, and D. H. Madison, J. Phys. B **40**, 3775 (2007).

[9]K. L. Nixon, A. J. Murray, O. Al-Hagan, D. H. Madison, and C. Ning, J. Phys. B **43**, 035201 (2010).
[10]L. R. Hargreaves, M. A. Stevenson, and B. Lohmann, Meas. Sci. Technol. **21**, 055112 (2010).
[11]L. R. Hargreaves, M. A. Stevenson, and B. Lohmann, J. Phys. B **43**, 205202 (2010).
[12]K. L. Nixon, C. Kaiser, and A. J. Murray, J. Phys. B **43**, 085202 (2010).
[13]J. Gao, D. H. Madison, and J. L. Peacher, J. Chem. Phys. **123**, 204314 (2005).
[14]J. Gao, D. H. Madison, and J. L. Peacher, Phys. Rev. A **72**, 032721 (2005).
[15]J. Gao, D. H. Madison, and J. L. Peacher, J. Chem. Phys. **123**, 204302 (2005).
[16]C. Lee, W. Yang, and R. G. Parr, Phys. Rev. B **37**, 785 (1988).
[17]C. F. Guerra, J. G. Snijders, G. te Velde, and E. J. Baerends, Theor. Chem. Acc. **99**, 391 (1998).
[18]S. J. Ward and J. H. Macek, Phys. Rev. A **49**, 1049 (1994).
[19]J. B. Furness and I. E. McCarthy, J. Phys. B **6**, 2280 (1973).
[20]J. P. Perdew and A. Zunger, Phys. Rev. B **23**, 5048 (1981).
[21]N. T. Padial and D. W. Norcross, Phys. Rev. A **29**, 1742 (1984).
[22]G. Purohit, A. S. Bhullar, and K. K. Sid, Indian J. Phys., B **77**, 177 (2003).
[23]G. Wannier, Phys. Rev. **90**, 817 (1953).
[24]S. A. C. Clarke, T. J. Reddish, C. E. Brion, E. R. Davidson, and R. F. Frey, Chem. Phys. **143**, 1 (1990).